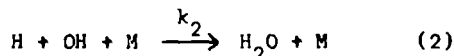
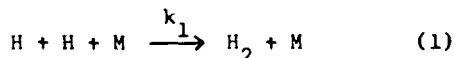


Kinetic Studies of Hydroxyl Radicals in Shock Waves. IV  
Recombination Rates in Rich Hydrogen-Oxygen Mixtures

Garry L. Schott and Paul F. Bird

University of California, Los Alamos Scientific Laboratory  
Los Alamos, New Mexico

Previous work<sup>1,2,3</sup> in rich hydrogen-oxygen-diluent flames has shown that in the final stage of the combustion reaction, several reversible reaction steps are maintained substantially in equilibrium, while net progress is achieved by the removal of excess species through three-body recombination reactions. The reversible reactions couple the recombination paths, so that each recombination reaction has the same degree of nonequilibrium (ratio of equilibrium constant to the quotient of the activities of products and reactants), and a single measurement serves to determine the chemical composition. Kinetics studies in such flames<sup>3,4</sup> have shown that the important recombination reactions are:



and have provided values of the rate coefficients  $k_1$  and  $k_2$  under flame conditions.

Observations on this reaction system in shocked gas mixtures have been reported in earlier papers of the present series,<sup>5,6,7</sup> and have indicated establishment of equilibrium conditions in the reversible reaction steps promptly at the end of the induction period. This paper reports measurements of the kinetics of the slow disappearance of OH following its maximum concentration in shocked  $\text{H}_2\text{-O}_2\text{-Ar}$  mixtures.

#### EXPERIMENTAL METHODS

Basic shock wave techniques and the ultraviolet line absorption method of determining OH concentration have been discussed in Part I<sup>5</sup>. However, many modifications of apparatus and procedures have been incorporated in the present work, and it is appropriate to present the methods used in this investigation.

The dimensions of the circular shock tube were: internal diameter, 10 cm throughout; driver chamber length, 192 cm; test chamber length, 373 cm. Its construction was of brass, and the interior surface of the test chamber was plated with nickel to decrease its porosity. Single and multiple layer brass shim stock diaphragms were used. Evacuation of the test chamber was accomplished through a side port located 13 cm from the diaphragm position. Final evacuation was done with an NRC B-2 oil diffusion-ejection booster pump backed by a Kinney KC 5 mechanical pump. Vacuum measurements in the test chamber were made with a CVC Philips gauge connected to a side port midway along its length.

Shock velocity measurement was made by a series of five deposited platinum resistor gauges. These gauges were 1 mm by 6 mm and had resistances between 30 and 200  $\Omega$ . They were flush mounted with the shorter dimension disposed axially

at intervals of 60.00, 50.00, 30.00, and 29.94 cm, beginning 198 cm from the diaphragm. The gauge outputs were amplified, shaped by 2D21 thyatrons, echoed after 6.25  $\mu$ sec, mixed with 10  $\mu$ sec timing marks, and presented on an oscilloscope raster<sup>8</sup> operating at 100  $\mu$ sec/line. A modified Tektronix 545 instrument was used.

The quartz windows for the light beam used in measuring OH concentrations were located 1.3 cm downstream from the fourth velocity gauge, some 34 cm from the end of the shock tube. This setup allowed several hundred microseconds for observation of the moving gas behind the incident shock wave before the arrival of the reflected wave from the end plate or the hydrogen driver gas from upstream.

The optical train from the flash discharge lamp to the photomultiplier detector was mounted independently of the shock tube. The flash lamp was operated in the way described in Part I<sup>5</sup>. The lamp itself differed, however, in that the  $H_2O$  vapor pressure was regulated at 0.9 mm Hg by  $NaC_2H_3O_2 \cdot 3H_2O + NaC_2H_3O_2$  at 0°C.<sup>2</sup>

At this working pressure the luminosity was much freer of spurious fluctuations in intensity than at higher pressures, and its intensity was only slightly diminished. A 2.5 cm focal length spherical lens immediately in front of the lamp focused the luminous region inside the toroidal anode crudely at the monochromator entrance slit 70 cm away, providing condensation of the beam in the (vertical) direction along the 2 mm by 10 mm collimating slits on either side of the shock tube windows. The luminous region itself was substantially as wide as the slits. At the monochromator entrance slit a crude  $f = 1.0$  cm cylindrical lens was used with its axis parallel to the slit to condense the beam onto the entrance slit and provide for filling the width of the grating. The 1P28 photomultiplier detector was placed immediately outside the exit slit of the monochromator.

The anode resistor used was 22 K  $\Omega$ , and 4 ft of RG-71 cable delivered the signal to the input terminal of a type L preamplifier in a Tektronix type 545 oscilloscope. Thus the electronic response time was about 2  $\mu$ sec, which approximately matches the time inhomogeneity in the gas sample within the 2 mm width of the beam. Faster response can be achieved, but for recombination rate measurements over periods like  $10^{-4}$  seconds it is unnecessary, and reduction in statistical noise is achieved by relaxing the time resolution.

The oscilloscope photographs contained, in addition to the light transmission record, a base line of zero photoelectric signal, and in displaced positions, a trace bearing timing marks and a trace of the unabsorbed photoelectric signal from a separate flashing of the lamp. This monitor trace was synchronized with the lamp firing in the same way as in the experimental trace. It was needed because the lamp signal, while reproducible in shape, was not quite constant over the time of the experiment.

The JACO model 8200 monochromator was operated in an air thermostat at  $36 \pm 1^\circ C$ . The first order spectrum was used with the entrance slit width 0.050 mm and the exit slit width 0.570 mm. The instrument was calibrated with a low pressure mercury discharge spectrum and set to transmit (ideally uniformly) between  $3088.7 \leq \lambda_{air} \leq 3097.3 \text{ \AA}$ , with transmission decreasing linearly to zero at  $3087.9 \text{ \AA} \leq \lambda_{air}$  and  $3098.1 \text{ \AA} \leq \lambda_{air}$ . Precision of the calibration and thermal stability are estimated at  $\pm 0.3 \text{ \AA}$ . Photographic spectra made with film held against the exit slit confirmed the isolation of the lines<sup>9</sup> between  $R_2 20$  ( $\lambda_{air} = 3089.0 \text{ \AA}$ ) and  $Q_2 8$  ( $\lambda_{air} = 3096.8 \text{ \AA}$ ).

Experimental gas mixtures were prepared manometrically from commercial cylinder gases in a thoroughly evacuated glass-lined (domestic hot water) tank and heated from beneath to be mixed by diffusion and convection for at least 24 hours before use. Mass spectrographic analysis of each batch confirmed the absence of unintended components beyond traces of  $N_2$  and  $CO_2$ .

## DATA REDUCTION

The raw data obtained in each experiment consist primarily of the recorded initial conditions, the shock velocity data contained in the photograph from the raster oscilloscope, and the OH concentration data contained in the oscilloscope photograph of the photoelectric signal. Prior to any chemical kinetics analysis these data are reduced to the apparent OH concentration as a function of time under particular conditions of temperature, pressure, and concentrations of other species. These preliminary data reduction procedures are discussed first.

### Shock Velocity

Evaluation of the shock wave velocity from the gauge positions and shock arrival times was done by adjusting each time for small differences in circuitry response (corrections of a few tenths of a microsecond), fitting the five  $x, t$  data points to the quadratic expression  $t = a + bx + cx^2$ , and evaluating  $(dt/dx)^{-1}$  at the observation window position. Except in shots at 15 and 20 cm Hg initial pressure,  $c$  was invariably positive, and the average attenuation of the shock velocity was about 1% per meter (0.1% per tube diameter). The heavier diaphragms used for the higher pressure shots apparently opened more slowly and sometimes caused the shock velocity to reach its maximum further downstream<sup>10</sup>. From least squares treatment, the indicated uncertainty in  $b$ , which is most of the uncertainty in  $dt/dx$ , was usually a few tenths of a percent. In a few cases it was as great as 1%, indicating irregular behavior of the shocks and/or the detection system.

### Hugoniot Calculations

Solution of the Rankine-Hugoniot equations was carried out by means of a computer code<sup>11</sup> to obtain the temperature, density, and composition behind each shock wave as functions of the initial conditions, the shock velocity, and the progress of chemical reaction. The computations for equilibrium conditions were obtained straightforwardly by the general method of Brinkley<sup>12</sup> which is incorporated in the shock equations code. The restricted equilibrium computations for selected extents of recombination less than the final equilibrium extent were made by arbitrarily constraining<sup>13</sup> the number of moles per original mole of material in the system. The species  $\text{Ar}$ ,  $\text{H}_2$ ,  $\text{O}_2$ ,  $\text{H}_2\text{O}$ ,  $\text{OH}$ ,  $\text{H}$ , and  $\text{O}$  were considered in the computations. Ideal gas thermodynamic functions for  $\text{H}_2$ ,  $\text{O}_2$ ,  $\text{H}_2\text{O}$ ,  $\text{OH}$ , and  $\text{O}$  were obtained from the JANAF tables<sup>14</sup> and formulated for interpolation in the polynomial form used previously in this<sup>11</sup> and other<sup>15</sup> laboratories.  $\text{Ar}$  and  $\text{H}$  were treated as calorically perfect and the coefficients were evaluated accordingly.

### Determination of [OH]

The calibration curve relating absorbance and OH concentration used in the earlier work was an empirical one based on observations of equilibrium gases in shock waves. For the present work, a much more refined method has been developed. It is a semi-empirical method based in part on absorbance measurements in equilibrium shocked gas, but it makes use of the fundamental molecular properties of OH to extend the calibration to regimes of OH concentration, temperature, and pressure where equilibrium observations could not be made.

The calibration program consists of three parts: (1) experimental determination of the spectral intensity distribution of our OH line source, (2) formulation of the absorption spectrum of OH on the basis of theory and integrated absorption coefficients derived from independent experiments, and (3) numerical synthesis of the response of thermal absorber to the lamp spectrum in order to account, within existing uncertainty in the absorption spectrum parameters, for the experimentally determined absorbance of equilibrium mixtures. The details of these steps are being reported separately; the methods used and their application to the old, higher

pressure lamp spectrum are described elsewhere<sup>16</sup>. The principal features of the calibration are summarized as follows. The line shapes and relative intensities in the lamp spectrum were determined from high dispersion photographic spectrograms made by repeated flashes. The source spectrum and the absorber spectrum were each described in the computations by superposition of lines having combined Doppler and Lorentz broadening<sup>17</sup>. The line strengths given by Dieke and Crosswhite<sup>9</sup> as modified by Learner<sup>18</sup> were used. The values of the transition probability coefficient,  $F$ , and the pressure broadening parameter,  $a$ , (as defined in the literature<sup>19</sup>) found to describe suitably the measured equilibrium absorbances were  $F = 3.50 \times 10^{-4}$  and  $a = 335 P(\text{atm})/T(^{\circ}\text{K})$ . These values are in reasonable agreement with those reported elsewhere<sup>19,20</sup>. Perhaps the present calibration is not significantly more accurate than the old empirical one in the regime where the latter was determined, but the extension to other regimes is superior, and the whole calibration is on a much firmer basis.

The computer program generates the absorbance ( $-\log_{10}$  of the fractional transmission) of the incident spectrum for a specified absorber temperature, pressure, and optical density (product of OH concentration and path length). Points covering the ranges of these parameters involved in the experiments were assembled and a numerical interpolation scheme was used to derive the OH concentration for a series of absorbance values during each experiment. For this purpose an average temperature and pressure for each experiment was obtained as the mean of the values computed for partial equilibrium conditions with zero recombination and complete equilibrium conditions. The absorbance for each optical density in the table was first interpolated to the appropriate temperature and then the appropriate pressure. Finally the several measured absorbances were interpolated to optical densities and hence OH concentrations. A quadratic interpolation formula was used in each step, with two of the three values of the independent variable bracketing the desired value.

#### Rate Equation

The rate equation for the disappearance of OH in a reacting mixture of  $\text{H}_2$ ,  $\text{O}_2$ ,  $\text{H}_2\text{O}$ , OH, H, and O is developed for conditions of variable density shock wave flow in a manner which incorporates the recombination mechanism, reactions (1) and (2), and anticipates the insertion of partial equilibrium relationships among the several species. Let us define the mole number of each species,  $n_i$ , by the relationship

$$\rho n_i = [I] \quad (3)$$

where  $\rho$  is the density in grams per liter and  $[I]$  is the concentration of species I in moles per liter. We then identify the partial derivative with respect to time ( $\partial[I]/\partial t$ ) =  $\rho dn_i/dt$  as the net volumetric rate of chemical production of species I<sup>21</sup>.

Now it has been shown that<sup>1,2,22</sup> in the system being considered, equating the total volumetric rate of production of all species to the combined chemical recombination rate from all paths,  $R_{\text{recomb}}$ , leads to

$$\rho d(n_{\text{H}} + n_{\text{OH}} + 2n_{\text{O}} + 2n_{\text{O}_2})/dt = -2 R_{\text{recomb}} \quad (4)$$

To formulate  $n_{\text{H}}$ ,  $n_{\text{O}}$ , and  $n_{\text{O}_2}$ , and their derivatives in terms of the measured  $[\text{OH}]$ , we proceed as follows. Let

$$[\text{OH}] = \alpha [\text{H}]. \quad (5)$$

Then

$$n_{\text{OH}} = \alpha n_{\text{H}} \quad (6)$$

and

$$\rho dn_H/dt = (\rho/\alpha) dn_{OH}/dt - (\rho n_{OH}/\alpha^2) d\alpha/dt. \quad (7)$$

Similarly let

$$[O] + [O_2] = \beta [OH]^2, \quad (8)$$

so that

$$n_O + n_{O_2} = \beta n_{OH}^2 \quad (9)$$

and

$$\rho d(n_O + n_{O_2})/dt = 2\beta n_{OH}^2 dn_{OH}/dt + \rho^2 n_{OH}^2 d\beta/dt + \beta \rho n_{OH}^2 d\rho/dt. \quad (10)$$

The scale of time,  $t$ , experienced by an element of shocked gas is converted to the scale  $\tau$  at an observation point stationary with respect to the unshocked gas by

$$dt = (\rho/\rho_0) d\tau \quad (11)$$

where  $\rho_0$  is the density of the unshocked gas.

The variables  $\rho$ ,  $\alpha$ , and  $\beta$  are considered as functions of the independent variable  $[OH]$ . Then from the definition, equation (3), it follows that

$$\rho dn_{OH}/dt = d[OH]/d\tau (1 - d \ln \rho / d \ln [OH]) \quad (12)$$

Finally, for conditions in which the recombination mechanism consists of reactions (1) and (2) and all dissociation rates are negligible, we express the total recombination rate,  $R_{\text{recomb}}$ , in terms of concentrations and conventional rate coefficients by

$$R_{\text{recomb}} = k_1 [M_1][H]^2 + k_2 [M_2][H][OH] \quad (13)$$

where  $[M_1]$  and  $[M_2]$  are the total gas concentrations acting as third bodies in recombination reactions (1) and (2).

Then substitution of equations (5) - (13) into equation (4) and rearrangement of terms leads to

$$\begin{aligned} \rho d(1/[OH])/d\tau = & 2(\rho/\rho_0) k_1 [M_1] \left(1 + \frac{\alpha k_2 [M_2]}{k_1 [M_1]}\right) \\ & \left\{ (1 + \alpha + 4\alpha\beta[OH])(1 - d \ln \rho / d \ln [OH]) - d \ln \alpha / d \ln [OH] \right. \\ & \left. + 2\alpha\beta[OH](d \ln \beta / d \ln [OH] + d \ln \rho / d \ln [OH]) \right\}^{-1}. \end{aligned} \quad (14)$$

For convenience we now refer to the factor 2 and the complicated expression in braces on the right hand side of equation (14) as  $A$ , and for lack of information to the contrary, identify the third body concentrations  $[M_1]$  and  $[M_2]$  with the total gas concentration,  $[M]$ . Thus the rate coefficients are referred to the experimental gas mixture, and we re-write the rate equation as

$$\rho d(1/[OH])/d\tau = A (\rho/\rho_0) [M](k_1 + \alpha k_2) \quad (15)$$

Equation (15) has been cast in this form in anticipation of finding the disappearance of OH to be effectively second order in OH and of determining the slope of an approximately linear plot of  $1/[OH]$  versus  $\tau$  from each experiment.

## RESULTS

Experiments have been done with three different gas mixtures, whose compositions are given below:

Mixture Designation	%H <sub>2</sub>	%O <sub>2</sub>	%Ar
R-1	4.03	1.00	94.97
R-2	2.02	0.50	97.48
R-3	8.07	1.00	90.93

The results of thirty-one experiments in the temperature range  $1400^\circ \leq T \leq 2000^\circ \text{K}$  are assembled in Table I. In these experiments, the plots from which  $d(1/[\text{OH}])/dt$  was determined were approximately straight over the entire interval plotted, which in most cases was from about 50  $\mu\text{sec}$  to about 500  $\mu\text{sec}$  after passage of the shock front. During this period  $[\text{OH}]$  fell from the values given in column 3 to those given in column 4. Column 5 contains the slopes derived from the plots. Columns 6 and 7 contain the values of  $[\text{OH}]$  and temperature computed from the initial data and shock velocity for each experiment on the basis of equilibrium with respect to all reactions except dissociation-recombination reactions and no change in the total mole number  $n = \sum n_i$ , from the value  $n_0$  in the unshocked gas mixture. Implicit in these computations are the relationships:

$$\alpha = [\text{OH}]/[\text{H}] = K_{18}[\text{H}_2\text{O}]/[\text{H}_2] \quad (16)$$

and

$$\beta = ([\text{O}] + [\text{O}_2])/[\text{OH}]^2 = K_{19}/[\text{H}_2\text{O}] + K_{20}/[\text{H}_2] \quad (17)$$

where  $K_{18}$ ,  $K_{19}$ , and  $K_{20}$  are the equilibrium constants for the reactions



and



Complete conversion of the initial O<sub>2</sub> to H<sub>2</sub>O with no production of OH, H, or O corresponds to final values of  $n/n_0$  of 0.990 in mixtures R-1 and R-3 and 0.995 in mixture R-2, and computations show that  $[\text{OH}]$  varies approximately linearly with  $n/n_0$ .

To interpret  $d(1/[\text{OH}])/dt$  by equation (15) for conditions prevailing early in the recombination reaction, computations were made of partial equilibrium conditions with  $n/n_0 = 1.000$  and  $n/n_0 = 0.999$ . The values of  $[\text{M}]$ ,  $\alpha$ ,  $(\rho/\rho_0)$ , and  $\beta$   $[\text{OH}]$  were taken as the means of these two computations, and the logarithmic derivatives which appear in the factor A were approximated from the finite differences between these two computations.  $[\text{M}]$  and  $\alpha$  so evaluated are listed in columns 8 and 9 of Table I.  $(\rho/\rho_0)$  was invariably between 3.2 and 3.6. The factor A varied systematically from 1.7 to 1.0 as  $\alpha$  varied from 0.01 to 0.1.

The derived values of  $k_1 + \alpha k_2$  given in the last column of Table I were obtained from the measured slopes in column 5 by multiplication by the factor  $\alpha \rho / \rho [\text{M}] A$ . The following values of  $k_1$  and  $k_2/k_1$  have been derived by linear least squares fitting of the entire set of values of  $k_1 + \alpha k_2$  in Table I and the indicated subsets thereof.

Group of Experiments				$k_1$	$k_2/k_1$
T range (°K)	[M] range mole/liter $\times 10^3$	Mixtures	No.	$\frac{\text{liter}^2 \text{mole}^{-2} \text{sec}^{-1}}{\times 10^{-8}}$	
1400-2000	8-36	All	31	6.6	7.1
1400-1700	8-36	All	17	6.1	11.4
1700-2000	9-30	All	14	5.9	8.5
1400-1700	8-10	R-1, R-3	6	5.6	17.8
1400-1700	17-19	R-1, R-3	7	6.1	9.5
1700-2000	9-10	R-1, R-3	6	6.6	7.7
1700-2000	17-19	R-1, R-3	4	4.9	14.0

We conclude that  $k_1$  in an atmosphere consisting primarily of argon is  $6 \pm 1 \times 10^8 \text{ liter}^2 \text{mole}^{-2} \text{sec}^{-1}$  between 1400° and 2000°K, and that  $k_2/k_1 = 10 \pm 5$  under these same conditions. No variation of either  $k_1$  or  $k_2/k_1$  with temperature can be established. When the points are plotted, a small trend toward lower apparent rate coefficients at higher values of [M] or [OH] is shown between the groups of points in mixtures R-1 and R-3 with  $[M] = 9 \times 10^{-3} \text{ mole/liter}$  and  $[M] = 18 \times 10^{-3} \text{ mole/liter}$ . However, this trend is not consistently borne out by the few experiments at still higher densities or the rather scattered data from mixture R-2. Such a trend may or may not be due to a small systematic error in the OH absorption spectrum calibration.

To be sure, significant departure of  $\alpha$  from the assumed partial equilibrium value of  $K_{18} [\text{H}_2\text{O}]/[\text{H}_2]$  would lead to serious error in the rate coefficients deduced. However, the available data<sup>23</sup> on the rates of the bimolecular reaction paths by which this equilibrium is approached indicate that  $\alpha$  does not depart from its ideal value by more than one percent under the conditions of the present experiments. Departure of [O] and [O<sub>2</sub>] from their assumed equilibrium relationship to [OH] would be less serious in the rich mixtures studied here.

The composition of the gas acting as the third body in the present work differs greatly from that which has been used in any of the other studies in this system, and the rate coefficients determined cannot be compared in detail. The values found here are generally lower than those reported<sup>3,4</sup> in mixtures composed primarily of H<sub>2</sub>, N<sub>2</sub>, and H<sub>2</sub>O. Within our own experiments, the only component of [M] to vary appreciably and systematically as  $\alpha$  was varied is [H<sub>2</sub>], which was about eight times as large (after formation of H<sub>2</sub>O, H, and OH) in the experiments with mixture R-3 as in those with mixture R-2. If H<sub>2</sub> were markedly more efficient than Ar in catalyzing reactions (1) and (2), the apparent rate coefficients at lower  $\alpha$  would be increased, producing higher  $k_1$  values and lower  $k_2/k_1$  values. Other workers<sup>3,4</sup> have not found evidence for marked efficiency of H<sub>2</sub> as third body.

#### GASDYNAMIC INSTABILITY

Nine additional experiments were attempted at temperatures between 1100° and 1300°K. These yielded apparent rate coefficients which scattered between 50% and 200% of those found above 1400°K. In several of these experiments, particularly those at higher densities, there were undulations of the OH absorption record and other indications of spin-like instability in the flow behind the shock wave. Investigation of this behavior is outside the scope of the present paper. However it may well be that such instabilities are in fact present in the higher temperature experiments, but their scale is evidently fine enough not to disrupt the kinetics dramatically.

Table I  
Summary of Experimental Results

Concentrations are in moles/liter, times in seconds, temperatures in °K, and velocities in km/sec.

Mix	Shock Velocity (obs'd.)	[OH] x 10 <sup>6</sup> (obs'd.) initial final	$\frac{d(1/[OH])}{dt}$ x 10 <sup>-9</sup>	[OH] x 10 <sup>6</sup> (calc'd.)	T (calc'd.)	[M] x 10 <sup>3</sup> (calc'd.)	$\alpha$ x 10 <sup>2</sup> (calc'd.)	(k <sub>1</sub> + $\alpha$ k <sub>2</sub> ) x 10 <sup>-8</sup>
R-1	1.226	5.2 2.5	.80	6.64	1546	8.84	4.49	10.5
R-1	1.232	5.1 2.2	.68	6.87	1560	8.87	4.65	9.3
R-1	1.251	7.2 2.4	.75	7.56	1599	8.92	5.13	11.3
R-1	1.396	14.2 4.5	.42	13.78	1921	9.31	9.71	12.1
R-1	1.408	13.0 3.5	.37	14.35	1949	9.34	10.15	11.4
R-1	1.417	16.9 4.1	.37	14.81	1972	9.36	10.50	11.8
R-1	1.200	6.9 1.8	1.47	11.57	1494	17.52	3.89	8.4
R-1	1.223	11.0 1.2	1.39	13.12	1541	17.67	4.43	9.0
R-1	1.275	14.0 1.4	1.05	16.97	1651	17.99	5.79	9.0
R-1	1.293	17.1 2.2	1.09	18.40	1689	18.09	6.31	10.2
R-1	1.385	26.7 2.9	.88	26.54	1896	18.58	9.33	12.3
R-1	1.388	28.2 2.9	.74	26.80	1903	18.59	9.42	10.4
R-1	1.196	13.4 0.6	3.23	22.58	1485	34.99	3.80	9.0
R-2	1.209	3.4 2.1	.65	3.27	1543	8.79	4.42	7.0
R-2	1.345	6.6 2.8	.55	6.04	1844	9.15	8.52	12.4
R-2	1.362	6.4 3.5	.28	6.44	1885	9.19	9.14	6.8
R-2	1.381	13.6 2.5	.64	13.80	1931	18.46	9.86	8.6
R-2	1.184	5.9 0.5	3.53	8.21	1490	25.21	3.81	11.1
R-3	1.247	1.8 0.6	2.31	2.20	1525	8.97	1.26	6.2
R-3	1.253	2.1 0.7	2.76	2.28	1537	8.99	1.31	7.6
R-3	1.279	2.4 0.7	2.35	2.69	1589	9.07	1.53	7.3
R-3	1.408	3.9 1.1	1.56	5.32	1863	9.43	2.97	8.2
R-3	1.409	4.6 1.4	1.37	5.35	1866	9.44	2.99	7.3
R-3	1.417	4.9 1.3	1.63	5.55	1884	9.46	3.10	8.9
R-3	1.185	2.2 0.3	7.84	2.85	1405	17.53	.835	7.8
R-3	1.212	2.7 0.4	5.64	3.47	1457	17.72	1.01	6.4
R-3	1.217	2.7 0.4	4.91	3.59	1466	17.75	1.04	5.7
R-3	1.396	6.9 1.1	2.66	10.09	1838	18.81	2.82	6.7
R-3	1.399	7.2 1.0	2.74	10.21	1843	18.82	2.85	7.0
R-3	1.348	8.7 0.4	4.63	12.79	1733	29.92	2.23	6.0
R-3	1.229	4.7 0.4	11.1	7.76	1488	35.65	1.12	6.8



## ACKNOWLEDGMENTS

The authors acknowledge gratefully the participation of Mr. John G. Williamson and Mr. James L. Young in the performance of the experiments and Mr. Michael P. Eastman in the measurement of the photographic records.

## REFERENCES

1. Bulewicz, James, and Sugden, Proc. Roy. Soc. (London) A235, 89 (1956).
2. W. E. Kaskan, Combust. Flame 2, 229 (1958).
3. Dixon-Lewis, Sutton, and Williams, Discussions Faraday Soc. 33, 205 (1962).
4. E. M. Bulewicz and T. M. Sugden, Trans. Faraday Soc. 54, 1855 (1958).
5. Bauer, Schott, and Duff, J. Chem. Phys. 28, 1089 (1958).
6. G. L. Schott and J. L. Kinsey, J. Chem. Phys. 29, 1177 (1958).
7. G. L. Schott, J. Chem. Phys. 32, 710 (1960).
8. H. T. Knight and R. E. Duff, Rev. Sci. Instr. 26, 257 (1955).
9. G. H. Dieke and H. M. Crosswhite, J. Quant. Spectr. Radiative Transfer 2, 97 (1962).
10. D. R. White, "Influence of Diaphragm Opening Time on Shock-Tube Flows", General Electric Research Laboratory Report No. 58 RL 1999, June, 1958.
11. Bird, Duff, and Schott, Los Alamos Scientific Laboratory Report LA 2980, 1964.
12. S. R. Brinkley, Jr., J. Chem. Phys. 15, 107 (1947).
13. G. L. Schott, J. Chem. Phys., accepted for publication, 1964.
14. JANAF Interim Thermochemical Tables, The Dow Chemical Company, Midland, Michigan, December, 1960, and Supplements through December, 1962.
15. Eschenroeder, Boyer, and Hall, Phys. Fluids 5, 615 (1962).
16. P. F. Bird, "Absorbance of the OH Radical in a Specific Wavelength Interval near 3090Å", Thesis, University of New Mexico, Department of Physics, 1961.
17. S. S. Penner, "Quantitative Molecular Spectroscopy and Gas Emissivities", Addison-Wesley, Reading, Massachusetts, 1959, Sections 3-5 and 4-4.
18. R. C. M. Learner, Proc. Roy. Soc. (London) A269, 311 (1962).
19. T. Carrington, J. Chem. Phys. 31, 1243 (1959).
20. W. E. Kaskan, J. Chem. Phys. 31, 944 (1959).
21. S. S. Penner, "Chemistry Problems in Jet Propulsion", Pergamon Press, New York, 1957, Section 72.
22. W. E. Kaskan and G. L. Schott, Combust. Flame 6, 73 (1962).
23. F. Kaufman and F. P. Del Greco, Ninth Symposium (International) on Combustion, Academic Press, New York, 1963, page 659.